Transition Met Chem (2010) 35:903–910
DOI 10.1007/s11243-010-9410-x

Hydrothermal and sonochemical synthesis of a nano-sized nickel(II) Schiff base complex as a precursor for nano-sized nickel(II) oxide; spectroscopic, catalytic and antibacterial properties

Lotf Ali Saghatforoush · Robabeh Mehdizadeh · Firoozeh Chalabian

Received: 5 June 2010 / Accepted: 9 August 2010 / Published online: 22 August 2010

Abstract The Ni(II) complexes $[Ni(L)_2](ClO_4)_2$ (**1**) and $[Ni(L)_2(NO_3)_2]$ (**2**), where L is the Schiff base ligand of 4,5,9,13,14-pentaaza-benzo[b] triphenylene, were synthesized and characterized by physico-chemical and spectroscopic methods. Nano-sized particles of (**1**) were prepared both by sonochemistry (**3**) and solvothermal (**4**) methods. NiO nanoparticles were obtained by calcination of the nano-structure complexes at 500 °C. The structures of the nano-sized compounds were characterized by X-ray powder diffraction and scanning electron microscopy. The thermal stabilities of the bulk complexes (**1–2**) and nano-sized particles (**3–4**) were studied by thermogravimetric and differential scanning calorimetry. The catalytic activities of complexes of (**1–4**) are reported. The free Schiff base and its Ni(II) complexes have been screened for antibacterial activities against three Gram-positive bacteria. The metal complexes are more active than the free Schiff base. Electrochemical studies show that the Ni complexes undergo irreversible reduction in MeCN solution.

Introduction

Schiff bases are widely employed ligands that exhibit various denticities and functionalities [1]. 1,10-Phenanthroline-5,6-dione (pdon) is a versatile ligand for the assembly of metal organic materials. It can be used directly as a bis-chelating ligand and be prepared starting from an already complexed phenanthroline. The diketone functionality can also easily be transformed to other chelating groups such as a diamine or a dioxime. Moreover, it is also a versatile organic linker that can form bridges through amine condensation or a combination of coordination and condensation [2]. Owing to its redox activity, pdon in both a metal-free state and in complexes with transition metals (ruthenium, cobalt, osmium, iron, and nickel) shows strong electrocatalytic activity for the oxidation of NADH. Many condensation reactions between the o-quinoid moiety of pdon and a diamine group have been reported [3]. 5,6-Diamino-1,10-phenanthroline (Phen-diamine) is particularly important in that it can either directly bridge two metal atoms or be condensed with a variety of ortho-quinones to form derivatives. For example, the useful bridging ligand, tetrapyrido[3,2-a:2′,3″,2″-h:2‴,3‴-j]phenazine (tpphz), is readily formed upon condensation of phen-diamine with pdon [4, 5]. Some Schiff bases have antibacterial, antifungal and antitumor activities [6–8]. The complexation of Schiff bases with iron, copper, zinc and other metals influences their antimicrobial activity [9]. Since nickel is present in the active site of urease and its complexes are used extensively in the design and construction of new magnetic materials, the study of nickel compounds is of great interest in various aspects of chemistry [10].

The macroscopic properties of materials strongly depend on both the size and the morphologies of the microscopic particles they are made up from. This is especially true for materials with morphological features smaller than a micron in at least one dimension, which are commonly called nanoscale materials, or simply nanomaterials. In these materials, the ratio of surface area to volume is vastly increased when compared to compounds with larger grain sizes and quantum mechanical effects such as the “quantum

---

L. A. Saghatforoush (✉) · R. Mehdizadeh
Department of Chemistry, Faculty of Sciences, Payame Noor University (PNU), P.O. Box. 58168-45164, Khoy, Iran
e-mail: saghatforoush@gmail.com

F. Chalabian
Department of Biology, Islamic Azad University, Tehran North Campus, Tehran, Iran

size effect” begin to play a significant role. Most importantly, the electronic properties of solids are altered with such great reductions in particle size, but also a number of other physical properties such as catalytic activities change when compared to macroscopic systems [11, 12]. Thus, the synthesis and characterization of nano-structures with different particle sizes and morphologies are very important both from the viewpoint of basic science as well as for technological applications [12].

Nanoparticles have attracted great interest in recent years because of their interesting chemical and physical properties, which are different from those of either the bulk materials or single atoms [13]. Among these materials, metal oxide nanoparticles are of technological importance for solar cells, chemical sensors and liquid crystal displays [13]. Sonochemistry is the research area in which molecules undergo a reaction due to the application of powerful ultrasonic radiation (20 kHz–10 MHz) [14, 15]. Herein, we describe the synthesis and characterization of new nickel(II) complexes of a Schiff base ligand namely (4,5,9,13,14-pentaaza-benzo[b] triphenylene). Nano-sized structures as well as bulk compounds were prepared using sonochemical and solvothermal methods and we have compared the catalytic activity of both to evaluate the interesting and highly valuable influence of the particle size of the nickel catalysts upon their activity. NiO nanoparticles were obtained by calcination of the nano-structure complexes. The antibacterial activities of the Schiff base and its complexes are reported against the three Gram-positive bacteria.

Experimental

All reagents and olefins were purchased from Merck or Fluka and used as received. Solvents used for reactions were purified and dried by conventional methods [16]. Nickel(II) perchlorate hexahydrate was purchased from Aldrich. 1,10-Phenanthroline-5,6-dione was prepared according to the reported method [17]. Caution: The perchlorate salts reported here are potentially explosive and, therefore, should be handled with care.

FTIR spectra were recorded using KBr disks on a Shimadzu FTIR model Prestige 21 spectrometer. The ^{1}H and ^{13}C NMR spectra were recorded on a Bruker spectrospin Avance 400 MHz in $CDCl_3$, and chemical shifts are indicated in ppm relative to tetramethylsilane. Melting points were determined using an electrothermal apparatus and are uncorrected. Electrospray ionization mass spectra (ESI–MS) were measured on a Micromass Qtof YA 263 mass spectrometer. The UV–vis spectra in the 200–900 nm range were obtained in MeCN on a Perkin-Elmer lambda 25 spectrophotometer. Conductivity measurements were carried out in MeCN at room temperature using a Metrohm conductometer. TGA were obtained on a Mettler-Toledo TGA 851e at a heating rate of 10°Cmin^{-1} under a nitrogen atmosphere. DSC thermograms were obtained on a Mettler-Toledo DSC 822e module, which was calibrated with indium metal ($T = 156.6 \pm 0.3$, $\Delta H = 28.45 \pm 0.61$ Jg^{-1}). Samples of 2–5.8 mg in solid form were placed in aluminium pans (40 µl) with a pierced lid, and heated or cooled at a scan rate of 10 °C min^{-1} under nitrogen flow. Cyclic voltammograms (CVs) were obtained using an Autolab modular electrochemical system (Ecochimie, Ulterecht, The Netherlands) equipped with a PGSTAT 20 module and driven by GPES (Ecochimie) in conjunction with a three electrode system and a personal computer for data storage and processing. An Ag/AgCl (Saturated KCl)/3M KCl reference electrode, a Pt wire (counter electrode) and a glassy carbon working electrode (Metrohm 0.0314 cm^{2}) were employed for the electrochemical studies. Voltammetric measurements were performed at room temperature in MeCN solution with 0.1 M tetrabutylammonium perchlorate as the supporting electrolyte. The reaction products of oxidation were analyzed by an HB 5890B gas chromatograph equipped with an HB-5 capillary column (phenyl methyl siloxane 30 m × 320 µm × 0.25 µm) with flame-ionization detector. An ultrasonic generator (Dr. Hielscher UP400 S ultrasonic processor) equipped with an H22 sonotrode with diameter 22 mm, operating at 24 kHz with a maximum power output of 400 W, was used for the ultrasonic irradiation. The ultrasonic generator automatically adjusts the power level. X-ray powder diffraction (XRD) measurements were performed using a Philips diffractometer manufactured by X’pert with monochromatized CuKα radiation. SEM images were recorded using a Philips model XL30. For characterization with a scanning electron microscope, samples were gold coated.

Preparation of the Schiff base ligand (L)

A solution of 2,3-diaminopyridine (0.109 g, 1 mmol) in absolute ethanol (5 mL) was added to a solution of 1,10-phenanthroline-5,6-dione (0.21 g, 1 mmol) in absolute ethanol (10 mL) to give a brown solution that was gently refluxed for about 3 h, then cooled to room temperature. A black precipitate was removed by filtration, and the filtrate was concentrated on a rotary evaporator. The yellow precipitate thus obtained was filtered off, washed with cooled absolute ethanol and then recrystallized from chloroform and dried under vacuum. Yield: 0.81 g (60%). Anal. Found: C, 72.1. H, 3.3. N, 24.8. Calcd: C, 72.1. H, 3.2. N, 24.7%. m.p: 238 °C. FT-IR (KBr disk): 3053, 1620, 1602, 1588, 1574 cm^{-1}. ^{1}H NMR (400 MHz $CDCl_3$) δ_H: 9.73 (dd, 1H, $J = 1.8$, $J = 8.1$), 9.54 (dd, 1H, $J = 1.8$, $J = 8.1$), 9.35 (dd, 1H, $J = 1.9$, $J = 4$), 9.28–9.31(m, 2H), 8.67(dd, 1H, $J = 1.9$, $J = 8.5$), 7.87(dd, 1H, $J = 4$, $J = 8.5$), 7.82(dd, 1H, $J = 4.5$, $J = 8.2$), 7.8(dd, 1H, $J = 4.5$, $J = 8.1$). ^{13}C NMR ($CDCl_3$) δ_C: 123.39, 123.51, 124.82, 125.89, 126.17, 13315, 133.85, 136.94, 137.47, 141.13, 142.53, 147.13, 147.29, 148.78, 151.93, 152.12, 154.68. ESI–MS: $m/z = 283.09$ (100%). UV–vis (λ_{max}/nm): 374, 355, 302, 294, 264.

Preparation of the nickel complexes

General procedure: to an ethanol solution (5 mL) of nickel salt (perchlorate or nitrate) (0.5 mmol), an ethanol solution (10 mL) of L (0.283 g, 1 mmol) was added. The resulting solution was refluxed for 2 h and then left at room temperature. The product was removed by filtration, washed with cooled absolute ethanol and recrystallized from methanol or acetonitrile and dried in vacuo.

[Ni(L)$_2$](ClO$_4$)$_2$ (1), Yield: 0.24 g (58%). Anal. Found: C. 49.6, H. 2.2, N. 17.0, Calcd: C. 49.6, H. 2.2, N. 17.0%. m.p: 309 °C. IR (KBr disk): 3076, 1654, 1622, 1573, 1084, 625 cm^{-1}. $\Lambda = 222$ μS. UV–vis (λ_{max}/nm): 575, 374, 357, 302, 269.

[Ni(L)$_2$(NO$_3$)$_2$](2), Yield: 0.215 g (58%). m.p: 308 °C. CHN. Found: C. 54.6, H. 2.5, N. 22.5. Calcd: C. 54.5, H. 2.4, N. 22.4%. IR (KBr disk): 3076, 1634, 1619, 1590, 1492, 1356, 1211, 826 cm^{-1}. $\Lambda = 65$ μS. UV–vis (λ_{max}/nm): 760, 558, 374, 358, 300, 268.

Preparation of [Ni(L)$_2$](ClO$_4$)$_2$ (3) nano-structures by sonochemical method

Ten microliters of a 0.1 M solution of $Ni(ClO_4)_2.6H_2O$ in MeOH was positioned in a high-density ultrasonic probe, operating at 24 kHz with a maximum power output of 400 W. Into this solution, 10 mL of a 0.2 M solution of the ligand L was added dropwise. The obtained precipitate was filtered off, washed with methanol and then dried in air. Anal. Found: C. 49.6, H. 2.3, N. 17.0. Calcd: C. 49.6, H. 2.2, N. 17.0%. m.p: 308–309 °C. IR (KBr disk): 3076, 1654, 1622, 1573, 1084, 625 cm^{-1}.

Preparation of [Ni(L)$_2$](ClO$_4$)$_2$ (4) nano-structures by solvothermal method

$Ni(ClO_4)_2.6H_2O$ (0.182 g, 0.5 mmol) and ligand L (0.283 g, 1 mmol) were dissolved in EtOH (15 mL) or a mixture of H_2O and EtOH. The solution was charged into a Teflon-lined stainless steel autoclave and heated at 150 °C for 24 h. After the autoclave was cooled immediately to room temperature, the product was filtered off, dried and characterized. Anal. Found: C. 49.6, H. 2.2, N. 17.0. Calcd: C. 49.6, H. 2.2, N. 17.0%. m.p: 307–309 °C. IR (KBr disk): 3076, 1654, 1622, 1573, 1084, 625 cm^{-1}.

General oxidation procedure

Oxidation reactions were performed in a stirred round-bottom flask fitted with a condenser. The reactions were carried out in air with acetonitrile as solvent and H_2O_2 as oxidant. In a typical experiment, a mixture of 0.032 mmol catalyst, 10 mL solvent, 1 mmol olefin and 1 mmol *n*-octane as internal standard was prepared. After the mixture was heated to 30 °C, 0.5 mmol H_2O_2 was added. At appropriate intervals, aliquots were removed and analyzed immediately by GC. Oxidation product yields based on the starting substrate were quantified by comparison with *n*-octane.

Antibacterial activity tests

The in vitro activity tests were carried out using the well method [18]. The potencies of the components were determined against the three Gram-positive bacteria: *Streptococcus pyogenes* (RITCC 1949), *Staphylococcus aureus* (RITCC 1113) and *Bacillus anthracis* (RITCC 1036). Microorganisms (obtained from the enrichment culture of the microorganisms in 1 mL Muller–Hinton broth, incubated at 37 °C for 12 h) were cultured on Muller–Hinton agar medium. The inhibitory activity was compared with standard antibiotic, gentamicin (10 μg). After drilling wells on medium using a 6-mm cork borer, 100 μL of the solution of each compound was poured into the well. The plates were incubated at 37 °C overnight. The diameter of the inhibition zone was measured to the nearest millimeter. Each test was carried out in triplicate, and the average was calculated for inhibition zone diameters. A blank containing only methanol showed no inhibition in a preliminary test. The micro-dilution broth susceptibility assay was used for the evaluation of minimal inhibitory concentration (MIC). After incubation at 37 °C for 24 h, the first tube without turbidity was determined as the MIC.

Results and discussion

The mononuclear complexes (**1**) and (**2**) were obtained by the reaction of $Ni(X)_2$. $6H_2O$ (X=ClO_4, NO_3) with L (molar ratio = 1:2, Fig. 1a, b). The analytical data for complexes are in good agreement with the calculated values. The solid compounds were stable at room temperature in air. The ^{1}H NMR spectrum of the free Schiff base ligand in chloroform displays eight signals assigned to the aromatic protons of L.

The ^{13}C NMR spectrum of L in chloroform displays 17 distinct signals assigned to the aromatic carbon atoms. The infrared spectra of the free ligand and its complexes were recorded in the region 4000–400 cm^{-1}. The spectra of the complexes show a band at 1,634–1,654 cm^{-1}, attributable to the imine groups, but no bands due to ν(C=O) vibrations. The spectra exhibit medium bands at 1,619–1,622 cm^{-1} as expected for the ring vibrations of the coordinated phenanthroline and at 1,573–1,590 cm^{-1} as expected for pyridine [19]. The FTIR spectra of all the complexes, compared with the free ligand, indicate that the ν(C=N) band at 1,602 cm^{-1} is shifted to higher frequency by 20 cm^{-1} in the complexes, indicating that the ligand is coordinated to the metal through the nitrogen atom of the phenanthroline group [19]. The IR spectra of the perchlorate complexes showed absorptions attributable to perchlorate at approximately 1,084 and 622 cm^{-1} [20]. The lack of splitting of these bands suggests that the perchlorate anions are not coordinated [19]. The complex (**2**) shows bands at 1,492 cm^{-1} (ν_1), 1,356 cm^{-1} (ν_5), 1,211 cm^{-1} (ν_2), and 826 cm^{-1} (ν_6) indicating coordination of the nitrate groups [21, 22]. The separation of $\sim$136 cm^{-1} between ν_1 and ν_5 indicates unidentate coordination of the nitrate [21]. The molar conductivity data at room temperature show that complex (**1**) is a 1:2 electrolyte, while complex (**2**) shows non-electrolytic nature [23]. The absorption spectra of compounds (**1**) and (**2**) were studied in acetonitrile. All of the complexes exhibit three absorption bands at 250–270 nm and 350–380 nm, due to the ligand centered π–π* transitions [24] or charge transfer (CT) transitions. The presence of a band at 575 nm in the spectrum of complex (**1**), which is assigned to a d–d transition, suggests that the coordination geometry at the metal atom could be distorted from square planar [25]. The presence of d–d bands at 558 and 760 nm in the spectra of complex (**2**) can be assigned to octahedral geometry around the metal center [26].

Cyclic voltammograms (CVs) of complexes (**1**) and (**2**) were recorded in acetonitrile with 0.1 M tetrabutylammonium perchlorate as supporting electrolyte in the potential range −2 to +0.1 V. Complex (**1**) exhibits an irreversible redox processes with one oxidation ($E_a = -0.103$ V) and one reduction peak ($E_c = -0.601$ V) related to the Ni^{II}/Ni^{III} couple. In addition, in complex (**1**), anodic and cathodic peaks ($E_a = -0.71$ V and $E_c = -0.95$ V) are observed at nearly the same potential values as the corresponding free ligand and may be due to irreversible redox process of the ligand. Complex (**2**) exhibited one irreversible reduction peak related to the Ni^{II}/Ni^{I} couple in addition to the ligand peaks (Table 1).

Nano-structured complexes (**3** and **4**) were obtained by both ultrasonic irradiation in a methanol solution and solvothermal reaction in an ethanol solution. IR spectra of the nano-structures are indistinguishable from complex (**1**). Fig. 1c gives an overview of the methods used for preparation of the nano-structures and their conversion to NiO by calcination. The XRD pattern of bulk complex (**1**) is the same as those of complexes of (**3**) and (**4**) prepared by the sonochemical and solvothermal methods, respectively. The obtained data indicate that the compounds obtained by both hydrothermal and sonochemical processes have an amorphous phase. The size of the particles is 58–82 nm, which is in agreement with that observed by scanning

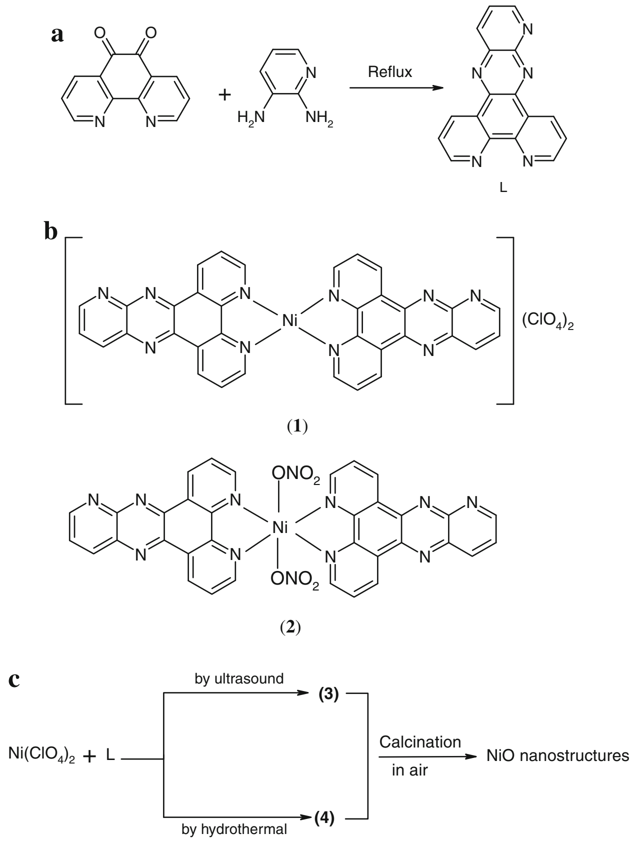

Fig. 1 (**a**) Syntheses and structure of the Schiff base ligand. (**b**) Suggested structures of Ni (II) complexes. (**c**) The formation of nanocompounds and synthetic methods

Table 1 Electrochemical data for nickel (II) complexes in CH$_3$CN solution

Complex	E_{pa}(V)	E_{pc}(V)	ΔE^a(mV)	i_{pa}/i_{pc}	$E^b_{1/2}$
(**1**)	−0.103	−0.601	498	0.46	−0.35
(**2**)	–	−0.677	–	–	–
(**3**)	−0.103	−0.601	498	0.53	−0.35
(**4**)	−0.112	−0.607	495	0.55	−0.35

Peak potentials $E_{1/2} = 1/2(E_{pa} + E_{pc})$

[a] $\Delta E_p = E_{pc} - E_{pa}$ at scan rate 100 mV

[b] Data from cyclic voltammetric measurements; $E_{1/2}$ is calculated as average of anodic (E_{pa}) and cathodic (E_{pc})

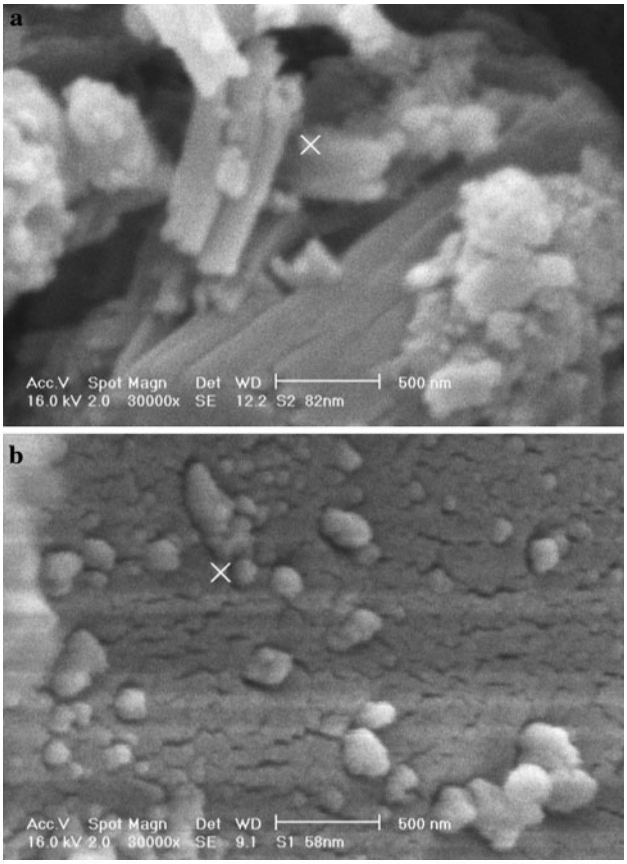

Fig. 2 SEM images of nano-structures: (**a**) complex (**3**) was prepared by ultrasound and (**b**) complex (**4**) was prepared by solvothermal

electron microscopy, as shown in (Fig. 2a, b). Thermal decomposition of the nano-sized structures of (**3** and **4**) in air at 500 °C produced NiO nano-structures as established by their powder XRD patterns (Fig. 3). The obtained patterns match with the standard patterns of face centered cubic NiO [27]. These nano-structures show the most crystallinity because of the existence of sharp peaks in the XRD pattern. The phase purity of the as-prepared face-centered cubic NiO nano-structures is completely obvious, and all diffraction peaks are perfectly indexed to the faced-centered cubic NiO structure with the lattice parameters of $a = 4.1769$ Å, $Z = 4$ and S.G = Fm3m in JCPDS card file No. 4-835. No characteristic peaks of impurities were detected in the XRD pattern. The broadening of the peaks indicated that the particles were of nanometer scale. Figure 4 shows an SEM image of the NiO nano-structures obtained from calcination of compound (**1**) under air.

To examine the thermal stabilities of the nano-sized structures and the corresponding bulk sample (**1**), thermal gravimetric analyses and differential scanning calorimetry were carried out between 25 and 850 °C in a static atmosphere of nitrogen. Enthalpy changes and decomposition temperatures of the free Schiff base and its nickel(II) complexes are tabulated in Table 2. The TGA data indicate that the nickel complex (**1**) start decomposition at 316 °C. There is no mass loss up to 200 °C, indicating that either water or solvent molecules are absent in these complexes. On the basis of the DSC data, the nano-sized structures of compounds (**3**) and (**4**) start to decompose at 285 °C and 289 °C, respectively.

For the catalytic investigations, we chose olefin oxidation, with the aim of obtaining epoxides as they are one of the most useful synthetic intermediates for the preparation of oxygen-containing natural products, epoxy resins and many others. Catalytic olefin epoxidation was performed at 30 °C under air in acetonitrile containing the olefin, oxidant and catalyst in a 1: 0.5: 0.032 M ratios. The only product of alkene oxidation by these systems was the

Fig. 3 XRD pattern NiO nano-structures

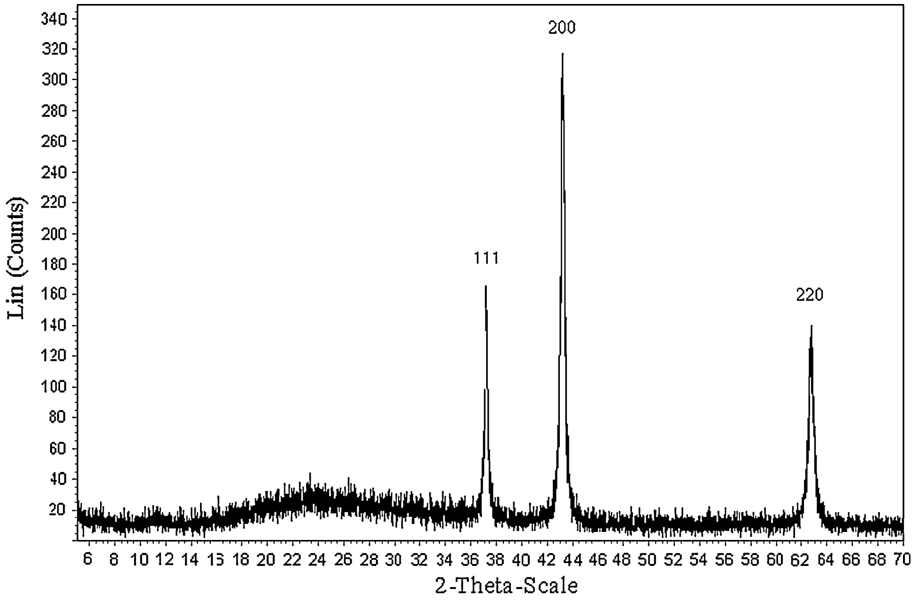

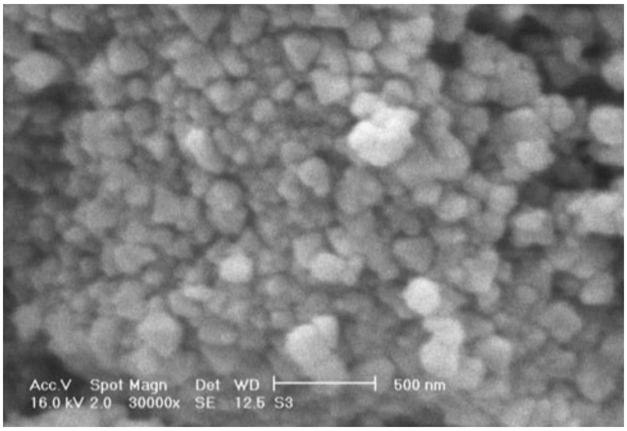

Fig. 4 SEM image of NiO nano-structures

Table 2 Thermoanalytical (enthalpy changes and decomposition temperatures) results of free Schiff base ligand and related Ni (II) complexes

Compound	T^a (°C)	ΔH^a(Jg^{-1})	T_d^b(°C)
L	238.32	16.93	299
(**1**)	316.83	47.79	320
(**2**)	314.35	54.15	320
(**3**)	284.57	73.82	290
(**4**)	286.31	74.26	290

[a] Data obtained from first DSC cycle

[b] Data obtained from TGA; 10 °C min^{-1} under N_2 gas

corresponding alkene oxide. The results of oxidation of alkenes and alkanes in the presence of these complexes as catalysts are summarized in Table 3. The final yields were typically obtained after 2 h. It can be seen that the nanosize catalysts are much more reactive than the parent bulk materials composed of micrometer or larger particles. Maximum conversion of alkenes or alkanes with the nanocatalysts is obtained within the first 5 min at room temperature. The presence of the oxidant H_2O_2 is essential for the reaction to proceed. The progress of olefin epoxidation catalyzed by these nickel complexes was investigated by UV–vis spectroscopy (Fig. 5). The initial spectrum changes after adding H_2O_2. The change in the spectra may be attributed to the rapid coordination of hydrogen peroxide to the nickel(II) and probably the reaction mechanism is improved via the formation of an intermediate oxo-metal species, as reported earlier for similar Schiff base complexes [28–31]. In the meantime, in order to check the stability of the catalysts in the reaction media, the IR spectra of the catalyst before and after the reaction were recorded. There were no differences in the IR spectra, hence the catalysts appear to be stable during the examination period [28–32]. Nitrogenous ligands are reported to lengthen and weaken the M–O bond in the oxidized form of the catalyst by donating electron density into the M–O antibonding orbital, which can account for the improved reactivity [33, 34].

Table 3 Epoxidation of alkenes and alkane with H_2O_2 catalyzed by Ni (II) complexes

	Conversion (%)		
Catalyst	Styrene oxide	4-methylstyrene oxide	Cyclooctanone
None	0	0	0
(**1**)	91.2	92.7	94.4
(**2**)	90	86	80
(**3**)	96.5	98	97
(**4**)	97	99	97

Conditions: catalyst, 0.032 mmol; substrate, 1 mmol; n-octane, 1 mmol; solvent, 10 mL; H_2O_2, 0.5 mmol, Temperature 30 °C, time reaction 2 h for bulk complex and first 5 min for nanocomplex

Antibacterial activities (zone of growth inhibition and minimal inhibitory concentrations) of the free Schiff base, its nickel complexes and of gentamicin (as a standard compound) are shown in Table 4. The organisms used in the present investigation were *Streptococcus pyogenes* (RITCC 1940), *Staphylococcus aureus* (RITCC 1885) and *Bacillus anthracis* (RITCC 1036) as Gram-positive bacteria. The data show that the free Schiff base has moderate activity against *S. pyogenes* and *S. aureus* and high activity toward *B. anthracis*. All of the Ni(II) complexes have strong activity against *S. aureus*, plus good activity (inhibitory

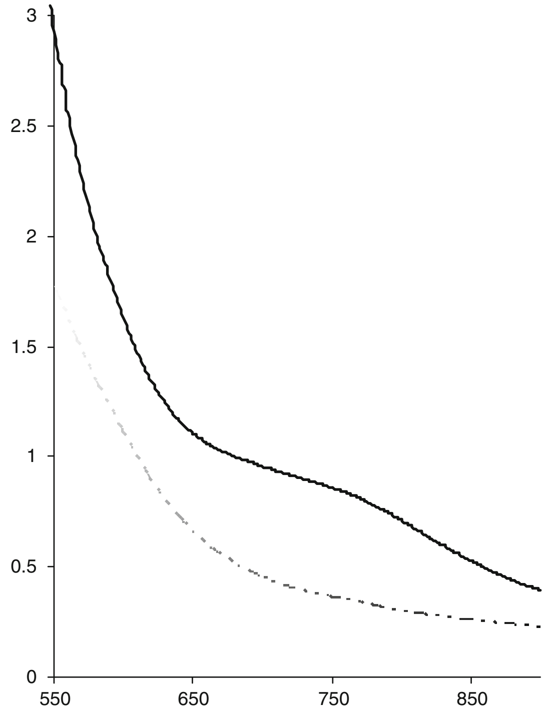

Fig. 5 Transition absorption spectrum (*solid line*) of complex (**1**), spectrum (*dotted line*) obtained after addition of H_2O_2 to complex (**1**)

Table 4 Antibacterial activities (zone of growth inhibition and minimal inhibitory concentrations) of Schiff base ligand and nickel (II) complexes and gentamicin (as a standard compound)

Method	Main compounds	Microorganisms		
		Streptococcus pyogenes (+)	*Bacillus anthracis* (+)	*Staphylococcus aureus* (+)
Growth inhibitory zone [mm]	L	16	25	17
	(**1**)	15	17	25
	(**2**)	17	20	29
	(**3**)	18	19	30
	(**4**)	20	20	30
Standard	gentamicin	13	32	13
Minimum inhibitory concentration (mg/ml)(MIC)	L	25	12.5	25
	(**1**)	25	25	12.5
	(**2**)	25	25	6.25
	(**3**)	25	25	6.25
	(**4**)	25	25	6.25

zones >15 mm) against *B. anthracis and S. pyogenes*. The antibacterial activities for the free Schiff base are lower than those for the complexes against *S. aureus* and *S. pyogenes*, except for complex (**1**) which has lower activity against *S. pyogenes*. [6]. In comparison with complex (**1**), the nanocomplexes (**3**) and (**4**) have good activity against all tested Gram-positive bacteria; this is probably because of the diminished the size of particle in these complexes**.** All the compounds exhibit greatest activity against *S. pyogenes* and *S. aureus* and among the complexes, the antibacterial activities of (**2**), (**3**) and (**4**) are the same. The quantitative assays gave MIC values in the region 6.25–100 mg mL^{-1} (Table 4), in agreement with the above obtained results.

Conclusion

The complexes [Ni(L)$_2$](ClO$_4$)$_2$ and [Ni(L)$_2$(NO$_3$)$_2$], where L is the Schiff base ligand of 4,5,9,13,14-pentaaza-benzo[b] triphenylene, have been prepared. Nano-sized complexes (**3**) and (**4**) were obtained by both ultrasonic irradiation in methanol solution and solvothermal reaction in ethanol, and characterized by physico-chemical, XRD and SEM techniques. Calcination under air of complexes (**3**) and (**4**) produce nano-sized structures of NiO. The antimicrobial activities show that the free Schiff base has moderate activity against three Gram-positive bacteria, while the Ni(II) complexes have moderate to strong activities. This is a scarce report of the synthesis of nano-sized structured Schiff base complexes and also nano-sized structures of NiO. The catalytic activity of bulk complex (**1**) and nano-structures (**3**) and (**4**) for the epoxidation of styrene, 4-methylstyrene and cyclooctane were tested. It was found that the tested complexes are effective catalysts, and the nano-sized complexes showed higher activities and shorter reaction times than the bulk complex.

Acknowledgments We are grateful to Payame Noor University for financial support of this work.

References

1. Maxim C, Pasatoiu TD, Kravtsov VC, Shova S, Muryn CA, Winpenny REP, Tuna F, Andruh M (2008) Inorg Chim Acta 361:3903
2. Larsson K, Öhrström L (2004) Inorg Chim Acta 357:657
3. Yokoyama K, Asakura T, Nakamura N, Ohno H (2006) Inorg Chem Comm 9:281
4. Boghaei DM, Behzadian-Asl F (2007) J Coord Chem 60:347
5. Hadadzadeh H, Olmstead MM, Rezvani AR, Safari N, Saravani H (2006) Inorg Chim Acta 359:2154
6. Saghatforoush LA, Chalabian F, Aminkhani A, Karimnezhad G, Ershad S (2009) Eur J Med Chem 44:4490
7. Shi L, Ge HM, Tan SH, Li HQ, Song YC, Zhu HL, Tan RX (2007) Eur J Med Chem 42:558
8. Saghatforoush LA, Aminkhani A, Chalabian F (2009) Transition Met Chem 34:899
9. Hothi HS, Makkar A, Sharma JR, Manrao MR (2006) Eur J Med Chem 41:253
10. Mukherjee P, Biswas C, Drew MGB, Ghosh A (2007) Polyhedron 26:3121–3128
11. Nalwa HH (2000) Handbook of nanostructured materials and nanotechnology, vol 1–5. Academic Press, Boston
12. Morsali A, Hossieni-Monfared H, Morsali A (2009) Inorg Chim Acta 362:3427
13. Askarinezhad A, Morsali A (2008) Mater Lett 62:478
14. Suslick KS, Choe SB, Cichowlas AA, Grinstaff MW (1991) Nature 353:414
15. Aslani A, Morsali A, Zeller M (2009) J Mol Struct 929:187
16. Perrin DD, Armarego WLF (1980) Purification of laboratory chemicals, 3edn. Pergamon, Oxford, pp 68, 174, 217
17. Yamada M, Tanaka Y, Yoshimoto Y, Kurda S, Shimao I (1992) Bull Chem Soc Jpn 65:1006
18. Baver A, Kirby WMM, Sherris JE, Turck M (1986) Am J Clin Pathol 45:493
19. Keypour H, Dehghani-Firouzabadi AA, Khavasi HR (2009) Polyhedron 28:1546
20. Ghosh M, Biswas P, Flörke U (2007) Polyhedron 26:3750
21. Shakir M, Azam M, Parveen S, Khan AU, Firdaus F (2009) Spectrochim Acta A 71:1851

22. Abd El-Wahab ZH, El-Sarrag MR (2004) Spectrochim Acta A 60:271
23. Szafran Z, Pike RM, Singh MM (1991) Microscale inorganic chemistry. Wiley, NewYork, p 104
24. Ilhan S, Temel H, Yilmaz I, Sekerci M (2007) J Organomet Chem 692:3855
25. Daneshvar N, Entezami AA, Khandar AA, Saghatforoush LA (2003) Polyhedron 22:1437
26. El-Tabl AS, El-Saied FA, Plass W, Al-Hakimi AN (2008) Spectrochim Acta A 71:90
27. Zhao ZW, Konstantinov K, Yuan L, Liu HK, Dou SX (2004) J Nanosci Nanotech 4:861
28. Pouralimardan O, Chamayou AC, Janiak C, Hosseini-Monfared H (2007) Inorg Chem Acta 360:1599
29. Koola JD, Kochi JK (1987) Inorg Chem 26:908
30. Mirkhani V, Moghadam M, Tangestaninejad S, Mohammadpoor-Baltork I, Shams E, Rasouli N (2008) Appl Catal A Gen 334:106
31. Chatterjee D, Mitra A (1999) J Mol Catal A Gen 144:363
32. Sheldon RA (ed) (1994) Metalloporphyrins in catalytic oxidations. Marcel Dekker, New York
33. Gold A, Jayaraj K, Doppelt P, Weiss R, Chottard G, Bill E, Ding X, Trautwein AX (1988) J Am Chem Soc 110:5756
34. Gunter MJ, Turner P (1991) J Mol Catal 66:121